Applied Catalysis B: Environmental 244 (2019) 983–995

Contents lists available at ScienceDirect

Applied Catalysis B: Environmental

journal homepage: www.elsevier.com/locate/apcatb

A systematic investigation on the bactericidal transient species generated by photo-sensitization of natural organic matter (NOM) during solar and photo-Fenton disinfection of surface waters

Mona Kohantorabi[a,b], Stefanos Giannakis[b], Mohammad Reza Gholami[a,*], Ling Feng[b,c], Cesar Pulgarin[b,**]

[a] Department of Chemistry, Sharif University of Technology, Tehran, 11365-11155, Iran
[b] School of Basic Sciences (SB), Institute of Chemical Science and Engineering (ISIC), Group of Advanced Oxidation Processes (GPAO), École Polytechnique Fédérale de Lausanne (EPFL), Station 6, CH-1015, Lausanne, Switzerland
[c] Ministry of Education Key Laboratory of Ecology and Resource Use of the Mongolian Plateau, School of Ecology and Environment, Inner Mongolia University, 010021, Hohhot, China

ARTICLE INFO

Keywords:
Advanced oxidation process (AOPs)
E. coli
Solar disinfection (SODIS)
Triplet state
Singlet oxygen

ABSTRACT

In this work, the role of dissolved oxygen in the solar and the photo-Fenton-mediated *E. coli* inactivation process was put under scrutiny. The effect of transient species that were produced in the presence of various natural organic matter isolates (NOM), namely Suwannee River (SR) NOM, Nordic Reservoir (NR) NOM, SR Humic acid (SRHA), and SR Fulvic acid (SRFA) was studied in detail. The role of $^1O_2$ in this reaction was systematically evaluated by modifying the O_2 concentration (N_2/O_2 purging) and the matrix composition (10, 50, and 100% deuterium oxide (D_2O) v/v). In the presence of NOM, $^1O_2$ was generated and the enhancement of *E. coli* inactivation rate due to charge transfer from triplet state to molecular oxygen. The comparison between SR and NR NOM showed that for these compounds, triplet state of NOM ($^3NOM^*$), and $^1O_2$ were the more favorable active species in *E. coli* inactivation, respectively. Also, the second order rate constants ($k^{2nd}_{E.coli}$) of *E. coli* with $^3NOM^*$, and $^1O_2$ were calculated by using the steady state approximation. The obtained results showed that the rate values of $^1O_2$ related to NR NOM was ~ 5.6 times higher than SR NOM, while the rate values of $^3NOM^*$ for SR NOM was ~ 8.7 times higher than NR NOM. We also determined the effect of these organic matter isolates in the photo-Fenton process and its constituents (solar/Fe^{2+}, solar/H_2O_2, and solar/Fe^{2+}/H_2O_2). In presence of NOM, the photo-Fenton process inactivation rates increased which confirmed that the combined processes has additional pathways generated with disinfecting effect during solar exposure of bacteria.

1. Introduction

The decrease of fresh water sources and the deteriorating water quality around the world are two of the most current environmental issues in global scale [1]. The unavailability or the inequality in global distribution of water, calls for a safe, easy, cheap, and highly efficient method for treating the available reserves, especially where means are scarce [2,3]. Among the various procedures to achieve this goal, solar disinfection (SODIS), which uses solar light for the purification of drinking water, has attracted high interest [4,5]. SODIS process has a proven efficacy, and an impressive impact whenever it was applied [1]. However, the most apparent contradiction lies within the fact that the scientific community has accepted it, the World Health organization (WHO) endorses it as a prevention method, but it is still rather poorly elucidated. Still the main factors which are agreed to be driving the inactivation process are the direct action of UVB (when transmitted through the reactor walls) [6], the indirect actions of UVA [7], temperature [8], and their synergies [9], but the natural presence of constituents such as metals (iron, and copper) or organic matter, can blur the understanding of the process [10,11].

Abbreviations: SODIS, solar disinfection; NOM, natural organic matter; ROS, reactive oxygen species; CT, charge transfer; PF, photo-Fenton; (LMCT), ligand-to-metal charge transfer; SR, Suwannee; NR, Nordic; FA, SR Fulvic acid HA; SR, humic acid; TOC, total organic carbon; PCA, plate count ager; LB, Luria-Bertani; EDC, electron donating capability; EDG, electron donating groups; SOD, superoxide dismutasc; ISC, intersystem crossing

* Corresponding author.
** Corresponding author.
E-mail addresses: gholami@sharif.ir (M.R. Gholami), cesar.pulgarin@epfl.ch (C. Pulgarin).

https://doi.org/10.1016/j.apcatb.2018.12.012
Received 7 July 2018; Received in revised form 27 October 2018; Accepted 3 December 2018
Available online 06 December 2018
0926-3373/

Natural organic matter (NOM) is a product of soil run-off, plant decay and plankton biomass, and is omnipresent in surface waters [12]. NOM has been recognized as a remarkable absorber of light and sensitizer that can produce reactive intermediates [13]. In these reactions, by absorbing the light, NOM acts as a primary chromophore which can influence photochemical transformations directly by bonding interactions, or indirectly through generating reactive oxygen species and other intermediates, including organic radicals. NOM is responsible for the generation of some reactive oxygen species (ROS) such as singlet oxygen($1O_2$) and superoxide ($O_2^{\bullet -}$), and other transient species, such as the triplet state of NOM($3NOM^*$), under the irradiation of solar light [14,15]. These species can reduce or oxidize compounds, leading to pathogens' inactivation and organic contaminants degradation [16,17].

Among of these species $^1O_2$ and $^3NOM^*$ are the important oxidants, causing the inactivation of bacteria [18]. In the presence of NOM the generation of $1O_2$is more probable via a charge transfer (CT) from triplet of NOM to molecular oxygen [19]. The photochemical and optical properties of these compounds are effective in facilitating CT [20]. This fact implies that on the one hand the presence of NOM is necessary, to get excited by light and on the other hand the critical role of oxygen concentration in this reaction in order to generate ROS [21].

The baseline damage of microorganisms can therefore be the predominant action of light on cells, as well as the indirect actions initiated by NOM. However, due to the presence of solar light, the disinfecting ability of this method can be enhanced by the addition of different oxidants, and catalysts [22,23]. The photo-Fenton (PF) processes (Fe^{2+}/H_2O_2/light, Eq. (1)) has attracted widespread interest during the last years [24]. This process can be used for degradation of pollutants, and inactivation of microorganisms in water and wastewater [25–27].

The opportunity of applying the photo-Fenton process where SODIS is applied is obvious. The main process, i.e. illumination, is present, hence the addition of the Fenton reagents would bring the desired enhancement effect. Although this process was considered to be effective mainly in acidic pH, due to the insolubility of ferric species, the success of this process at near-natural pH is based on the solar-mediated reduction of ferric aqua-complexes species, which are photo-active. Their reduction to Fe^{2+} enhances the efficiency of Fenton reaction according to Eq. (2) [20,28]. The ferrous iron re-participates in a photo-Fenton process in a self-catalytic cycle producing additional $HO^{\bullet}$.

$$Fe^{2+} + H_2O_2 \rightarrow Fe^{3+} + HO^{\bullet} + OH^- \quad (1)$$

$$Fe^{3+} + H_2O \xrightarrow{h\nu} Fe^{2+} + HO^{\bullet} + H^+ \quad (2)$$

Another important advantage of NOM in natural waters on photo-Fenton process is the facility to work at that natural pH [29,30]. Various organic compounds including carboxylic acids, and phenols have been shown as effective ligands for ferric complexes [31]. In presence of NOM the reaction efficiency of SODIS and photo-Fenton (PF) is enhanced, due to generation of active species. It can participate in the reaction with organic matter, and produce organic radicals, extra transients via the Ligand-to-Metal Charge Transfer (LMCT), hence the augmented inactivation potential at neutral pH (Eq. (3)) [32,33].

$$RCOO\cdots Fe^{3+} \xrightarrow{LMCT} Fe^{2+} + CO_2 + R^{\bullet +} \quad (3)$$

Nevertheless, there is a big correlation on the success of the SODIS and its enhanced version on the oxygen levels in the water prior to experimentation. Although for instance the epilimion (top layer of lakes) may be well oxygenated, the high temperatures that dominate the field and the SODIS process in PET bottles urged practitioners to recommend shaking the bottles before exposure; practically, absence of oxygen would mean no Reactive Oxygen Species (ROS) [34,35]. Literature lacks a work that focuses on the interplay among these two factors, which in fact, need one another to proceed to bacterial inactivation, although relevant works exist for viruses [36].

In this study, we focused on the role of O_2 and the dependence of bacterial inactivation with NOM, on the efficiency of SODIS and photo-Fenton. Also, we studied the effect of different kinds of NOMs including Suwannee River (SR) and Nordic Reservoir (NR) NOM, SR Fulvic Acid (SRFA), and SR Humic Acid (SRHA) on the solar disinfection process. The role of each transient species produced in this reaction was evaluated in details, and the kinetics of the reactions were investigated. The effect of the organic matter type, oxygen concentration matrix composition (as a method for ROS enhancement), and use of iron as a natural source of catalyst were in-depth evaluated. Finally, a similar approach has been performed for the photo-Fenton processes for bacterial inactivation, analyzed under different conditions of matrix and Fenton reagents' presence.

2. Materials and methods

2.1. Chemicals and reagents

Hydrogen peroxide solution (30% w/w), $FeSO_4$. $7H_2O$ (99%), furfuryl alcohol (FFA, 98%), 2, 4, 6, Trimethylphenol (TMP, 97%), acetonitrile (ACN, ≥ 99.9%), deuterium oxide (D_2O, 99.9% atom D), Select Yeast Extract, potassium chloride (99%), sodium chloride (99.5%), and ammonium molybdate tetrahydrate were purchased from Sigma Aldrich. Titanium (IV) oxysulfate solution and sodium iodide (< 99.5%) were obtained from Fluka. Tryptone was purchased from Bacton (Dickinson and company). Catalase from bovine liver (≥ 30,000 units/mg protein) and superoxide dismutase from bovine erythrocytes (≥ 3000 units/mg protein) were supplied from Sigma Aldrich. Suwannee River Natural Organic Matter (SR NOM, 2R101 N), Nordic Reservoir Natural Organic Matter (NR NOM, 1R108 N), Suwannee River Humic Acid (SRHA, 2S101 H) and Suwannee River Fulvic Acid (SRFA, 1S101 F) were purchased from the International Humic Substances Society. MilliQ water was used for the preparation of all solutions (~15.8 MΩ cm, Millipore Elix Advantage 3, and Millipore AG).

2.2. Analytical methods

2.2.1. Equipment

A UV–vis spectrophotometer (Varian Cary 100) was applied for absorption measurements. Also, the Total Organic Carbon concentration (TOC) of Natural Organic Matter solutions (NOM) was determined by Shimadzu A-200 TOC analyzer (Tokyo, Japan). The concentration of dissolved oxygen in reactions was evaluated by using an oxygen probe from Mettler Toledo (Switzerland). The concentrations of TMP, and FFA for kinetics calculation were obtained by high-performance liquid chromatography (HPLC).

2.2.2. Hydrogen peroxide quantification

The concentration of H_2O_2 was quantified during the reaction by the following methods:

i) Addition of $TiOSO_4$ solution:

After certain time intervals during the process, 1 mL of reaction solution was transferred into a cuvette, and 20 μL of $TiOSO_4$ solution were added. The absorption of this solution was measured by spectrophotometer at 410 nm

ii) Addition of sodium iodide (NaI) and ammonium molybdate ($(NH_4)_6Mo_7O_{24}$):

In this method, after certain time intervals, 300 μL of irradiated sample was transferred into the cuvette, and 675 μL of NaI solution [0.1 M], and 25 μL of ammonium molybdate [0.01 M] were added into the above mixture. After mixing for 5 min, the absorption of this solution was measured at 350 nm by the spectrophotometer.

2.2.3. FFA and TMP concentration

The concentration of FFA and TMP was determined by using HPLC with a UV detector set at detection wavelength of 215 nm. The mobile

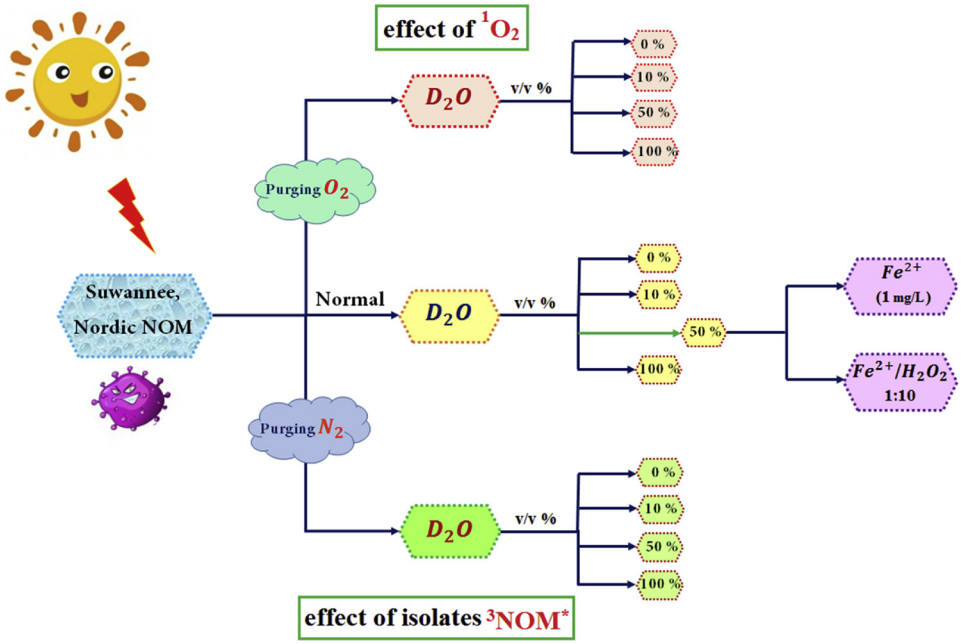

Fig. 1. Layout of the experimental plan of this study.

phase consisted of 30% acetonitrile (ACN) and 70% water, and was used at a 0.8 mL min^{-1} flow rate. For the detection of TMP concentration, the wavelength was set at 278 nm. The mobile phase for these samples was a mixture of 50% ACN and 50% water, while the flow rate was 1 mL/min.

2.3. Bacterial strain and inoculum preparation

All disinfection experiments were carried by using *Escherichia coli* strain K12 (DSMZ, No. 498), from the Deutsche Sammlung von Mikroorganismen und Zellkulturen) as an indicator of fecal contamination by bacterial species. The *E. coli* K12 strain was kept in cryovials containing 20% glycerol at −20 °C. At first, 20 µL of bacteria precultures spreading onto the Plate Count Agar (PCA), and then kept in an incubator at 37 °C for 24 h. Afterwards, a grown colony was spread on a new PCA plate and incubated for additional 24 h at the same temperature. After this time, the as-prepared master plate was stored at 4 °C.

For the working strain, a stock solution was made from the master plate. Firstly, Luria-Bertani (LB) solution (10 g/L Bacto™ Tryptone, 10 g/L NaCl, and 5 g/L Yeast extract) was prepared and then heat-sterilized in an autoclave. One bacterial colony from the master plate was inoculated into a sterile flask (25 mL) containing 5 mL of LB broth solution. This solution was agitated for 8 h at 200 rpm at 37 °C. Afterwards, 2.5 mL of this solution was added into a 500-mL flask containing 250 mL of LB broth. The flask was agitated at 200 rpm and 37 °C for 15 h to ensure stationary phase of the bacterial population. Finally, two samples (25 mL) were centrifuged (Hermle Z 323 K, Renggli Laboratory systems) at 4 °C, and 5000 rpm for 15 min. The obtained bacterial cells were washed twice with saline solution under the same conditions, at 4 °C. Finally, the bacterial pellets were re-suspended in 25 mL of saline solution and stored at 4 °C. The concentration of stuck solution by this procedure is approximately 10^9 CFU/mL.

In order to follow the bacterial population during the reaction, 100 µL of sample was dispersed onto a petri-dish containing PCA. In order to obtain a measurable count of colonies, the solution was 10-fold diluted in series before plating. The plate was kept for 24 h at 37 °C in an incubator, in the dark. All experiments were performed at least in duplicate under the same reaction conditions (biological replicate), in two parallel tests (statistical replicate), and at least two dilutions were plated.

2.4. Experimental procedure

Bacterial inactivation experiments were carried out in Pyrex glass bottle reactors under constant stirring at 350 rpm. A lab scale SUNSET solar system (Hanau) equipped with air-cooled Xenon lamp, and 650 W/m^2 solar intensity was applied for both solar and photo-Fenton experiments, in presence/absence of various NOM including, Suwannee (SR), Nordic (NR), Humic Acid (HA), and Fulvic acid (FA). The solar simulator was fitted with a filter with cut off lower than 290 nm. For the photo-Fenton experiments, 1 mg/L iron from a stock solution (1000 mg/L) was added to reactors and stirred, followed by addition of hydrogen peroxide in the solution (10 mg/L in the reactor) [37]; light was then provided to the system. After different intervals time, 1000 µL from the bulk solution were sampled and used for determination of bacterial concentration. For the preparation of NOM, a certain amount of each isolate was added in MQ-water, then pH was adjusted to 8.0. This solution was stirred at room temperature overnight, and stored at 4 °C. Before starting the experiments under different gases, the reactors were purged by N_2, or O_2 for 10 min.

2.5. Design of experimental plan

In principle, the experimental plan conceived to prove the role of oxygen concentration in the presence of NOM for bacterial inactivation reaction (Fig. 1). Under solar light, various transient species such as $^3NOM^*$, and$^1O_2$ can be generated and enhance bacterial inactivation. As such, the effect of different levels of O_2 are studied for both SR, and NR NOM. Also, after choosing the best concentration of each NOM, the role of singlet oxygen ($^1O_2$) from NR and SR NOM is investigated by addition of D_2O in the reaction. The kinetics of reactions were evaluated, and first order rate constants (k_{app}) were calculated. In addition, the second order rate constants of $^3NOM^*$, and $^1O_2$ are determined by using the steady-state approximation method. Finally, in order to evaluate the role of NOM in Fenton (Fe^{2+}), and photo-Fenton (solar/Fe^{2+}/H_2O_2) processes, theses reactions are carried out in the presence of SR and NR NOM. Due to presence of Fe^{2+}, and NOM in the reaction, the generation of Fe-NOM complexes is investigated and the overall effect of NOM constituents is presented.

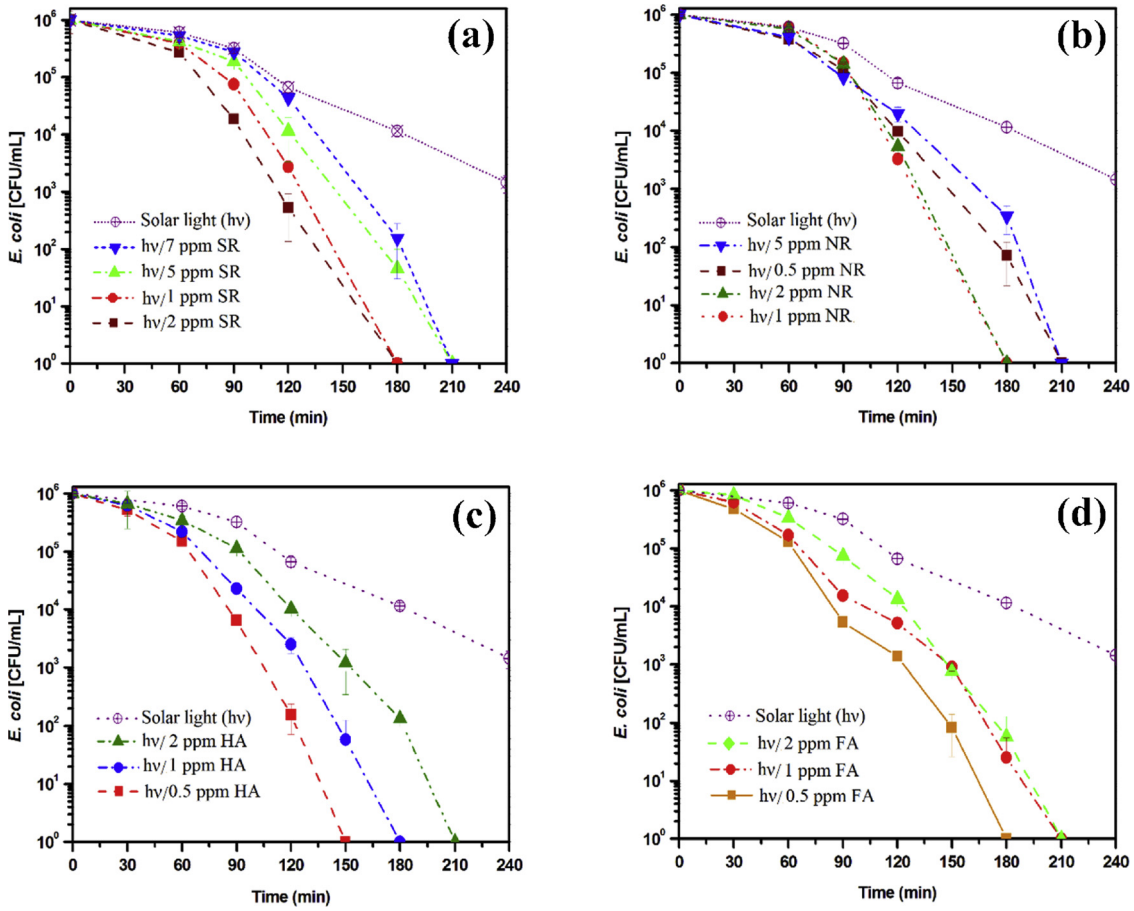

Fig. 2. Effect of Suwannee river (SR) (a), Nordic river (NR) (b), Humic acid (HA) (c), and Fulvic acid (FA) (d) concentration in bacterial inactivation reaction (light intensity: 650 W/m^2).

3. Results and discussion

3.1. NOM and O_2 influence on solar disinfection (SODIS)

In order to identify the role of NOM concentration and type, different addition levels were applied in this process for both NOM isolates (SR and NR NOM). According to these results, by increasing the concentration of SR and NR NOM, the apparent first order inactivation rate constant (k_{app}) values increased. The process reaches a plateau, from the competition of photons among NOM and bacteria, as well as the generated transients; self-inhibition and/or light attenuation is possible, hence the inactivation efficiency decreases after 2 mg/L for SR NOM and 1 mg/L for NR NOM (Fig. 2a, b).

The NOM used in the study contain variable concentrations of its constituents, some of which are the humic and fulvic acids. For SR NOM, the separate effect of SRHA and SRFA is presented in Fig. 2c, d. For these compounds, increasing the concentration demonstrated decreasing performance in bacterial inactivation. However, among the two, SRHA showed globally faster inactivation kinetics than SRFA. It should be noted that HA and FA have more phenolic moieties than SR NOM [38]. Also, the electron donating capability (EDC) for the different NOM enhances as following order: HA ~ FA < SR NOM [39]. These results indicated the high absorption capability of light for HA, and FA. Due to high light absorption, lower concentration of HA, and FA NOM requirements to achieve similar bacteria inactivation in the presence of SR NOM. Also, the UV–vis absorbance spectrum for the two isolates NOM (Figure S1, see Supporting information) indicated a notable difference among SR and NR NOM. In summary, the concentration of SR and NR NOM with the fastest kinetics obtained was 2 and 1 mg/L, respectively and subsequently applied in all further experiments, while the best concentration for HA, and FA NOM was selected at 0.5 mg/L.

By providing solar light to the system, various reactive species, including singlet oxygen($^1O_2$), superoxide ($O_2^{\bullet-}$), and hydrogen peroxide (H_2O_2) are expected to be produced. In the first step of this reaction, NOM absorbs solar light and gets excited to a triplet state($^3NOM^*$). Afterwards, singlet oxygen can be produced due to energy transfer between ($^3NOM^*$) and molecular oxygen. Then electron transfer reactions and an intermediate charge transfer (CT) complex with di-radical character is facilitated [40]. And finally, electron transfer between $NOM^{\bullet+/\bullet-}$ and O_2, lead to the generation of $O_2^{\bullet-}$ which can be converted to H_2O_2; a summary is provided in Eqs. (4)–(10):

$$^1_{NOM} + h\nu \rightarrow {}^1_{NOM^*} \rightarrow {}^1_{NOM^*} \quad (4)$$

$$^1_{NOM} + h\nu \rightarrow NOM^{\bullet+/\bullet-} \quad (5)$$

$$^1NOM^* \rightarrow NOM^{\bullet+/\bullet-} \quad (6)$$

$$^1NOM^* \rightarrow NOM^{\bullet+/\bullet-} \quad (7)$$

$$^3_{NOM^*} + O_2 \rightarrow {}^1_{NOM} + {}^1_{O_2} \quad (8)$$

$$^3_{NOM^*} + O_2 \rightarrow {}^1_{NOM} + {}^1_{O_2} \quad (9)$$

$$2O_2^{\bullet-} + 2H^+ \rightarrow H_2O_2 + O_2 \quad (10)$$

So NOM has a crucial part in this process. In order to identify the ROS generated in its presence, their amounts and their importance in the abovementioned bacterial inactivation, we modified the involved parameters, starting with the dissolved oxygen. Firstly, the dissolved oxygen of reaction was changed by purging nitrogen or oxygen into the reactors, to generate quasi-oxygen-free or oxygen-saturated

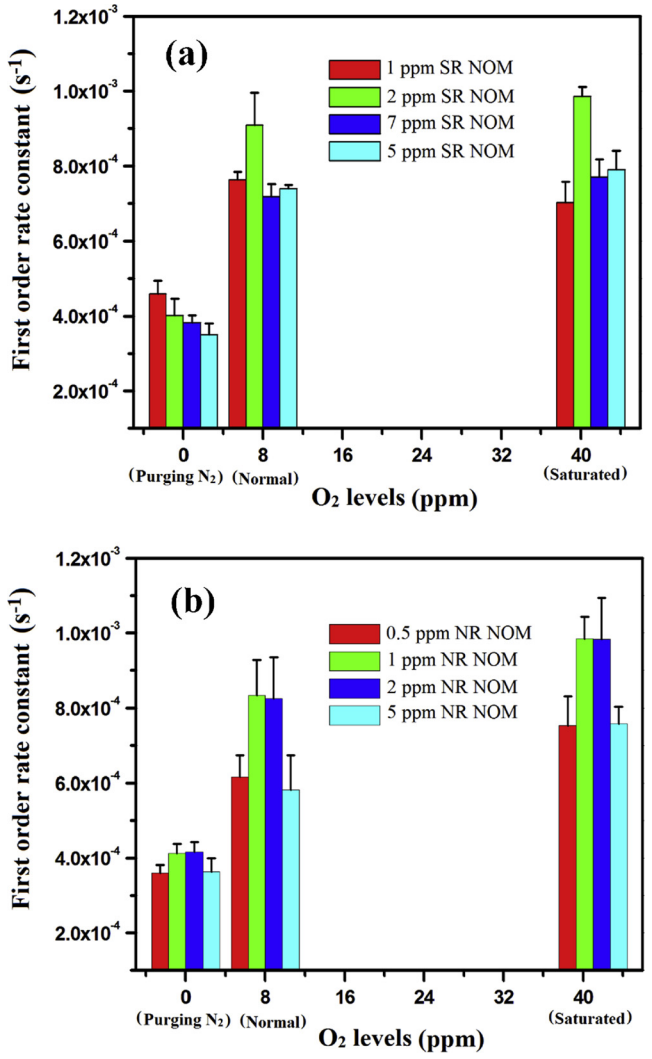

Fig. 3. Summary of the first order rate constant values for SR and NR NOM under different concentrations, and conditions (Purging N_2, and O_2, light intensity: 650 W/m^2).

environments, and thus study the role of $^1O_2$ in these processes. Fig. 3 summarizes the difference in kinetics as a function of the dissolved oxygen in the matrix. As it can be seen from the obtained results (a detailed description of kinetics is provided in Figures S2, and S3), by purging N_2 as a method to remove (most of the) oxygen from the system, the role of $^1O_2$ species was reduced in this process, and the rate constant was decreased. On the contrary, increasing the dissolved oxygen by purging O_2 in reactions, the efficiency of bacterial inactivation increased. The same behavior was observed for both SR and NR NOM; always the O_2-saturated environment was faster than the oxygen-deprived environments; at the best concentrations of SR and NR NOM, total disinfection (about 6-log decrease in bacterial population) took place at around 180 min. Hence the important point now would be to evaluate the difference among the NOM isolates and their response in the different environments.

As can be seen from the plots in Fig. 3, purging O_2 enhances the role of singlet oxygen in presence of NR NOM, more than in presence of SR NOM. This behavior can be related to photochemistry of NOM [41,42]. However, before going further to elucidate the exact mechanism, as a first checkpoint, we can propose that different NOM leads to different inactivation patterns according to their reactivity with O_2. SR NOM seems to predominantly react with bacteria in its triplet state and NR NOM via the singlet oxygen pathway. In order to further assess the role and the importance, the generation and propagation of the transient species have to be distinguished. Although there is a lot of research related to NOM-O_2 interactions, the information about the optical and photochemical properties in relation with the ROS-generation capacity are still not clear. Here the evaluation proxy (bacterial inactivation) is even harder to evaluate. Different models such as charge transfer (CT) interaction has received much attention in recent years to explain the photochemical properties of NOM [38]. The observed properties of NOM are a result of multiple population of chromophores that their contribution is varied by molecular weight fraction [13]. Nevertheless, all processes generate transient species and a deeper look into the topic follows.

3.2. Reactive oxygen species (ROS) generation and contribution to E. coli inactivation

3.2.1. Role of $^1O_2$

Two of the most important species can be obtained by reaction of $^3NOM^*$ with O_2 are singlet oxygen and superoxide. The influence of $^3NOM^*$ and $^1O_2$ was investigated by purging nitrogen and oxygen in reactors before starting the reaction. By addition of dissolved oxygen in the system the rate constant of reactions increased that means the role of singlet oxygen in this reaction is important. Conversely, purging N_2 would isolate the bactericidal effect of $^3NOM^*$ alone. Hence so far, the obtained results confirmed that NR NOM produced $^1O_2$ more than SR NOM. Now, in the previous set-ups, modification of the reaction medium from H_2O to D_2O was effectuated to affect the $^1O_2$ pathways.

Singlet oxygen has a longer lifetime in the presence of D_2O compared to H_2O [43]. The decay time of $^1O_2$ in the normal water is 3.5 μs [44,45] which can increase in the presence of D_2O to 67 μs [46,47]. The efficiency of $^1O_2$ quenching in water is higher than D_2O. Due to the high quenching rates in water (2.5×10^5 s^{-1}) compared to D_2O (1.6×10^4 s^{-1}), the concentration of $^1O_2$ in D_2O should be higher than that in water [48]. Scrutinizing the role of $^1O_2$ required performing the reaction in presence of different amounts of D_2O (namely 10, 50, and 100% v/v). The first-order rate constant values of reaction were calculated and reported in Table 1.

At lower concentrations of D_2O (10%), in presence of either SR or NR NOM the reaction was only slightly faster than in water. More specifically, in absence of D_2O, the first order inactivation rate constants in the presence of SR and NR NOM are $(7.993 \pm 0.861) \times 10^{-4}$ s^{-1}, and $(8.337 \pm 0.951) \times 10^{-4}$ s^{-1}, respectively. As it can be seen from the obtained results (Table 1), by addition of D_2O (50%) into the reactions, these values increased similarly and reached to $(10.10 \pm 0.933) \times 10^{-4}$ s^{-1}, and $(10.30 \pm 0.872) \times 10^{-4}$ s^{-1}, and showed the best performance in this reaction, even compared with the assays in presence of 100% D_2O. To explain this phenomenon, it should be noted that, by the replacement of water with D_2O, there is a pathway that possibly gets affected, i.e. the generation of H_2O_2 would be decreased. The interaction of $^3NOM^*$ with O_2 can result to superoxide

Table 1
Influence of different concentrations of D_2O (0, 10, 50, and 100% v/v) in the presence of SR (a), and NR (b) NOM on rate constant values of bacterial inactivation.

D_2O (% v/v)	NOM	k_{app}^{1st} (s^{-1})
0	SR	$(7.993 \pm 0.861) \times 10^{-4}$
	NR	$(8.337 \pm 0.951) \times 10^{-4}$
10	SR	$(8.140 \pm 0.473) \times 10^{-4}$
	NR	$(8.459 \pm 1.132) \times 10^{-4}$
50	SR	$(10.10 \pm 0.933) \times 10^{-4}$
	NR	$(10.30 \pm 0.872) \times 10^{-4}$
100	SR	$(9.780 \pm 1.553) \times 10^{-4}$
	NR	$(10.102 \pm 0.805) \times 10^{-4}$

radical ($O_2^{\bullet-}$), and from that, H_2O_2 can be formed. In D_2O environments, this reaction is not favored due to the replacement of hydrogen (from water) with deuterium.

According to the energy difference between $^1O_2$ and triplet state of NOM, approximately 30–50 % of $^3NOM^*$ can contribute to formation of $^1O_2$ [13,38]. These reports imply and our results confirm that $^1O_2$ is one of the favorable active species in the presence of NOM along with $O_2^{\bullet-}$. It is known that the optical and chemical characteristics of NOM can affect the generation of reactive species. Due to presence of phenolic and electron donating groups (EDG) in SR NOM compared with NR NOM, which have a known photo-activity, the formation of transient species in SR NOM is more favorable (see IHSS Website). NR NOM has a high ability to produce $^1O_2$ [49], which is confirmed by the higher inactivation of bacteria in the presence of 50% D_2O (Table 1).

Furthermore, the concentration of dissolved oxygen during the nitrogen purging (or oxygen) into ultrapure water was measured at room temperature (Figure S4). After three minutes purging O_2 into the reactors, the concentration of dissolved oxygen reached to 42.12 mg/L, while after two minutes purging nitrogen, the concentration of oxygen reached 0.01-0 mg/L. It was also found that the presence of NOM does not affect the O_2 concentration (Figure S5). Furthermore, purging N_2, and O_2 in presence of D_2O was studied (Figure S6). The diffusion of molecular oxygen into the solution decreased and the values of dissolved oxygen in the reactors reached to 40.8, and 39.5 mg/L for 50%, and 100% D_2O, respectively. In Fig. 4, the bacterial inactivation tests performed in these conditions are summarized. As it can be seen, by purging O_2 into the reaction, the rate of inactivation increased for both of SR and NR NOM, although this increase for SR NOM is lower than NR NOM. This behavior indicated that singlet oxygen is a more active species for bacterial inactivation in presence of NR NOM. Indeed, the results for 1 mg/L NR, and 50% of D_2O present total *E. coli* inactivation within a period of 150 min (Fig. 4e). By purging O_2 into the system, higher inactivation than normal conditions was obtained. Under these conditions, the reaction including SR [2 mg/L] or NR [1 mg/L] NOM and 50% of D_2O achieved a total disinfection (6-log decrease) within 2 h, while at the experiments under N_2 environment the slowest inactivation was observed. By purging N_2 into the reaction, a similar behavior was obtained for all NOM isolates. For all experiments after 3 h, *E. coli* inactivation reaches only 3-log and confirms the critical role of singlet oxygen in this reaction as an important species that produced by reaction between $^3NOM^*$ and O_2.

The reaction temperature and dissolved oxygen values were evaluated during solar exposure (Figure S7). According to these results, reaction temperature increased from 21.8 °C to 29.1 °C within 3 h. The illuminated reaction leads to only a slight increase of the temperature of the solution, as the simulator has an air-cooling system. By this temperature increase, the dissolved oxygen was decreased from 8.68 mg/L to 7.2 mg/L. Although this difference here can be negligible, the high temperatures during solar disinfection in PET bottles in the field conditions might drastically reduce the O_2 concentration and hamper the $^1O_2$-mediated inactivation. However, in the abovementioned results, the $O_2^{\bullet-}$ could play a role which cannot be directly seen, hence further testing was initiated.

3.2.2. The role of $O_2^{-\bullet}$ and H_2O_2

To further evaluate the role of $O_2^{\bullet-}$, superoxide dismutase (SOD), which converts $O_2^{\bullet-}$ to H_2O_2, was added to reduce the $O_2^{\bullet-}$ concentration. The reaction was carried out under the same conditions as previously. Fig. 5a and b illustrates the obtained results for *E. coli* inactivation. These results confirmed that the concentration of $O_2^{\bullet-}$ in the presence of SR NOM is low. In fact, addition of SOD into the reactor does not induce any difference in the bacterial inactivation process. For these reactions 6-log bacterial decrease happens within 3 h. Addition of SOD into the reactions induced by NR NOM resulted in complete *E. coli* inactivation within 210 min (Fig. 5, b), i.e. slower than the original processes. Hence, NR NOM was found to be more favorable than SR NOM for electron transfer between $NOM^{\bullet+/\bullet-}$ and O_2 that produce superoxide as an active species for bacterial inactivation (Eq. 9). According to these results, $^3NOM^*$ and $^1O_2$ are, respectively, the most germicidal species in the presence of SR and NR NOM under light irradiation.

By superoxide dismutation, H_2O_2 can be generated during the reaction in the presence of NOM. According to Eq. (10), due to reaction between superoxide radicals with H^+, H_2O_2 can be obtained. For this reason, the *E. coli* inactivation after addition of catalase (CAT) into water was studied for SR and NR NOM (Fig. 5). From the obtained results, catalyzing H_2O_2 in the presence of SR NOM did not result in a notable change of the inactivation rate, which means that H_2O_2 is not a critical species for bacterial inactivation, or at least, in the concentration at which is generated in this time frame. However, by adding CAT in to the reaction containing NR NOM the time required to reach 6-log decrease in bacterial population was increased (210 min). This result is in agreement with the behavior of $O_2^{\bullet-}$ that can be converted to H_2O_2 in presence of NR NOM. Due to higher production of $O_2^{\bullet-}$ in this reaction with NR NOM isolate, the concentration of H_2O_2 should be higher. Summarizing, assessing the effect of $^3NOM^*$, $^1O_2$ and $O_2^{\bullet-}$ /H_2O_2, the former two are shown to play a more important role in bacterial inactivation, and $O_2^{\bullet-}$ /H_2O_2 mainly in presence of NR NOM.

3.3. Second order reaction rate constants calculation of transient species with E. coli

Literature has suggested different kinetic expressions that have been applied for bacterial and viral inactivation modelling [50,51]. Here, we began with the calculation of the inactivation rate constants. The results showcase the critical role of NOM in bacterial inactivation. The addition of any NOM isolate caused an increase in the rate of inactivation due to generation of more transient species, mainly $^3NOM^*$ and $^1O_2$. However, the quantification of the species in each NOM case still remains open. The effect of two important species including $^3NOM^*$, and $^1O_2$ that generation by irradiation of light in the presence of SR and NR NOM was investigated by the calculation of second order reaction rate constant. Due to interaction between solar light and NOM, singlet excited electronic state ($^1NOM^*$) produced which through intersystem crossing (ISC) can convert to $^3NOM^*$ (Eq. (13)). In order to evaluate the steady-state concentration of NOM^*, which is the first and main reactive species of NOM under irradiation, the degradation of 2, 4, 6-Trimethylphenol (TMP) was studied under the same reaction conditions in the presence of SR and NR NOM (Figure S8). This compound is non-biodegradable and doesn't have significant toxic effect on *E. coli*, at least at the concentrations used and for the (short) time-frame of experimentation.

The concentration of [NOM^*], and second order rate constant ($k^{2nd}_{E.\,coli-NOM}$) of the reaction were calculated by the following equations (Eqs. (11) and (12)):

$$[NOM^*]_{ss} = \frac{1}{k_{TMP}} \times \lim_{[TMP]\to 0}\left\{\frac{-d\,[TMP]}{dt} \times \frac{1}{[TMP]}\right\} \tag{11}$$

$$k^{2d}_{E.\,coli-NoM} = \frac{k^{1st}_{E.\,coli-NOM}}{[NOM^*]_{ss}} \tag{12}$$

In Eqs. (11) and (12), k_{TMP}, and $k^{1st}_{E.\,coli-NOM}$ are the reaction rates of $^3NOM^*$, which is estimated to be 1.6×10^9 M^{-1} s^{-1},[42] and the first order rate constants of bacterial inactivation in the presence of SR or NR NOM, respectively. The obtained values were reported in Table 2. It is clear that, among the two different NOM isolates, SR is more effective in producing $^3NOM^*$ than NR NOM; the second order rate constant for SR NOM is ~ 8.7 times higher than NR NOM.

Furthermore, the second order rate constant of $^1O_2$ were calculated in these reactions by following the degradation of FFA under the solar light and normal O_2 concentrations in the presence of SR or NR NOM. The following series of reactions is proposed for bacterial inactivation:

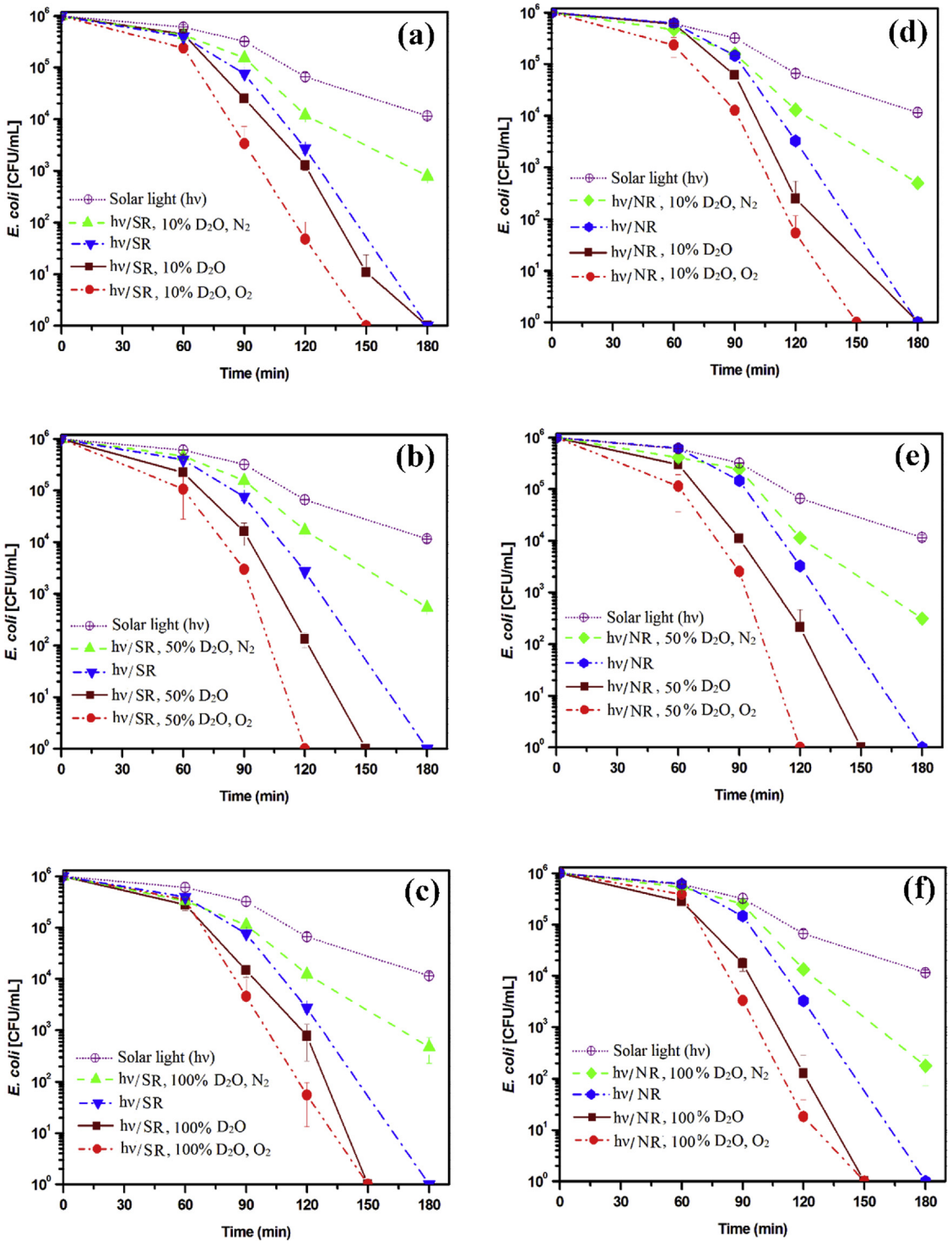

Fig. 4. Effect of different concentrations of D_2O (10, 50, and 100% v/v) in *E. coli* inactivation reaction in the presence of SR [2 mg/L], and NR [1 mg/L] NOM (light intensity: 650 W/m^2).

Under solar irradiation, by reaction between O_2 and $^3NOM^*$, $^1O_2$ can be produced (Eq. 14). This active species participated in bacterial (B) inactivation (Eqs. 15,16), and then converted into the normal oxygen by thermal deactivation (Eq. 17).

$$NOM \xrightarrow{h\nu} {}^3NOM^* \quad (13)$$

$$3_{NOM^*} + O_2 \rightarrow NOM + {}^1O_2 \quad (14)$$

$$B + {}^1O_2 \rightarrow Products\ [k_{E.coli,}{}^1{}_{O2}] \quad (15)$$

$$B + {}^3NOM^* \rightarrow Products\ [k_{E.coli}, {}^3N_{OM}{}^*] \quad (16)$$

$${}^1{}_{O_2} \rightarrow O_2\ [k_{17} = 2.5 \times 10^5 s^{-1}] \quad (17)$$

According to the steady-state approximation to calculate $^1O_2$, the following equation was used for the initial transformation rate of TMP (R_{TMP}) in the presence of bacteria.

$$R_{TMP} = \frac{R_{1O_2} \times k_{E.\,coli,\,{}^1O_2} \times [E.\ coli]}{k_{17} + k_{E.\,coli,\,{}^1O_2} \times [E.\ coli]} \quad (18)$$

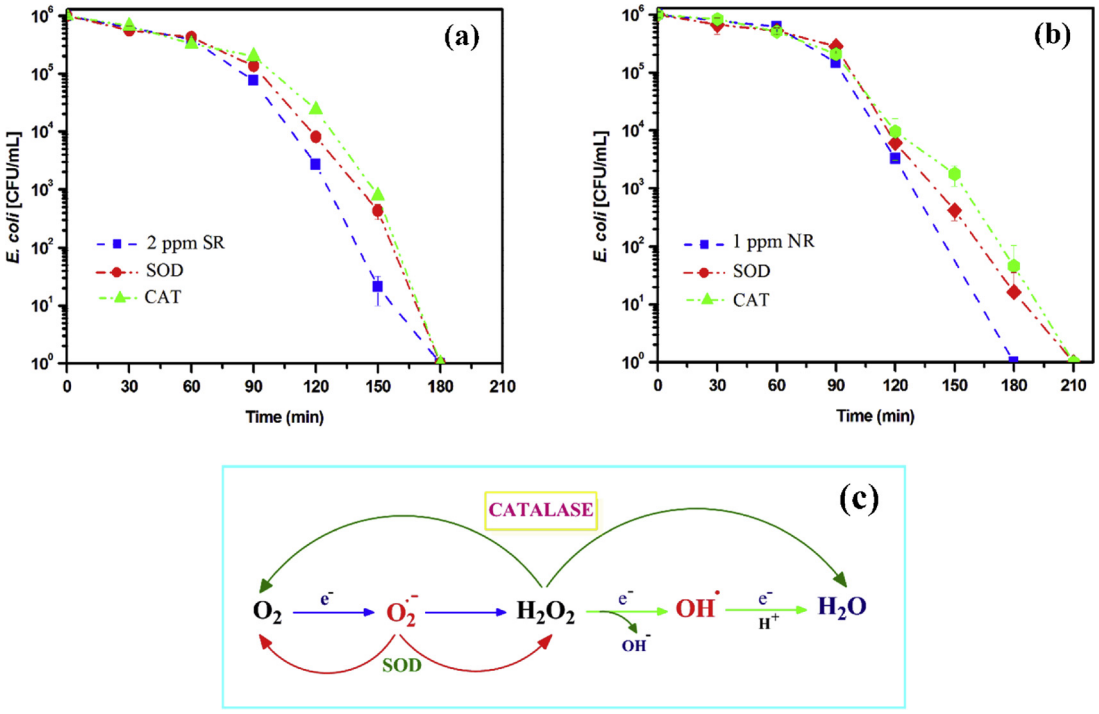

Fig. 5. *E. coli* inactivation in the presence of SR (a), and NR (b) NOM by addition of superoxide dismutase (SOD) and catalase (CAT) for the scavenging of $O_2^{\bullet-}$ and H_2O_2, respectively. Summary of the mechanism of converting transient species in the presence of SOD and CAT (c).

Table 2
The obtained values of second order rate constants of $^3NOM^*$, and $^1O_2$ for SR, and NR NOM isolates in *E. coli* inactivation.

$k^{2d}_{E.coli}$ (M^{-1} s^{-1})	SR NOM	NR NOM
$^3NOM^*$	(5.48 ± 0.62) × 10^{11}	(6.30 ± 0.51) × 10^{10}
$^1O_2$	(4.31 ± 0.60) × 10^6	(2.43 ± 0.80) × 10^7

R_{1O2} is the formation rate of $^1O_2$ in the presence of SR or NR NOM in the reaction under solar light. For the measurement of R_{1O_2}, the reaction was carried out upon irradiation of NR [1 mg/L] or SR [2 mg/L] NOM, and FFA [5×10^{-5} M] that reacts with $^1O_2$ with a rate constant 1.0×10^8 L mol^{-1} s^{-1} [52,53]. The initial transformation of FFA in the presence of NR, and SR NOM was (10.88 ± 0.18) × 10^{-11} M s^{-1}, and (8.35 ± 0.19) × 10^{-11} M s^{-1} respectively. Also, the photo-generated $^1O_2$ could undergo deactivation, or react with FFA. By using the steady-state approximation to [$^1O_2$], $R_{1O_2}$was calculated as follows (Eq. 19):

$$R_{1O_2} = R_{FFA} \times \frac{k_{17} + k_{FFA,\,^1O_2} \times [FFA]}{k_{FFA,^1O_2} \times [FFA]} \quad (19)$$

The second order rate constant for both NOM isolates was calculated and reported in Table 2. As it can be seen from the obtained results, NR NOM is confirmed to be more active in the generation of $^1O_2$. More specifically, the second order rate constant of $^1O_2$ for NR NOM is ~ 5.6 times higher than SR NOM. These results are in good agreement with the obtained results for purging O_2 into the reaction; due to formation of $^1O_2$ with high rate constant in the presence of NR NOM, by purging O_2 the rate constant value of *E. coli* inactivation increased. Also, the effect of D_2O in the presence of NR NOM, confirmed the activity of $^1O_2$ in this reaction. Finally, we have to comment here the values obtained and the proximity to the diffusion limit, as it is perceived in most of the studies with chemical contaminants. The difference of the size between the microorganism and the transient species in investigation is very large, hence the order of magnitude of the diffusion limit can be up to two orders of magnitude more [54]. Also, the high difference in these values can be explained if we take into account the durability of the target, i.e. the resistance of bacteria towards the transient species, which may contradict with the low difference in inactivation kinetics observed before. It has been found that, for instance for hydroxyl radical, around 10^9 $HO^{\bullet}$ are needed to inactivate a cell [50]. Hence, the evaluation proxy (bacterial cultivability) could be masking these differences.

3.4. Photo-Fenton processes: NOM and oxygen influence

3.4.1. Photo-Fenton inactivation of E. coli in absence of NOM

In order to investigate the effect of oxygen on the germicidal capacity of the photo-Fenton process (PF), bacterial inactivation in the absence of NOM was carried out by addition of Fe^{2+} or H_2O_2 alone and Fe^{2+}/H_2O_2. The obtained results are illustrated in Fig. 6. For the coupling of solar light (650 W/m^2) with Fe^{2+} [1 mg/L], the rate constant of bacterial inactivation increased and complete *E. coli* inactivation was achieved within 3 h. By addition of iron to the reaction, an

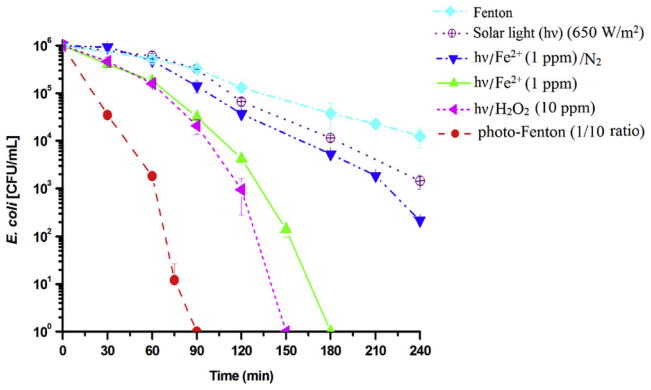

Fig. 6. *E. coli* inactivation using the Fenton reagents (without light), iron only, iron under purging N_2 into the reaction, and photo-Fenton process. (Fe^{2+} [1 mg/L], H_2O_2 [10 mg/L], and light intensity: 650 W/m^2).

enhancement occurs due to the i) transport of Fe into the cell, or ii) in the presence of dissolved molecular oxygen due to generation of superoxide and hydrogen peroxide (Eqs. (20), and (21) and iii) the reduction of Fe^{3+} to Fe^{2+} (Eq. (22)) with the hydroxyl ion as Lewis base.

$$Fe^{2+} + O_2 \xrightarrow{h\nu} Fe^{3+} + O_2^{\bullet -} \xrightarrow{H^+} H_2O_2 \quad (20)$$

$$Fe^{2+} + H_2O_2 \rightarrow Fe^{3+} + HO^{\bullet} + OH^- \quad (21)$$

$$Fe^{3+} + H_2O + h\nu \rightarrow Fe^{2+} + H^+ + HO^{\bullet} \quad (22)$$

Where Fe^{3+} refers to the photo-active aqua complexes in water, in the form of $Fe(OH)_x(H_2O)_y$.

Furthermore, the sole addition of H_2O_2 was very effective in reducing bacterial load, reaching total inactivation in 150 min. H_2O_2 poses an extra problem in the ROS balance inside the cell, fueling an intracellular photo-Fenton process [55]. Nevertheless, the process is presented only as an intermediate step to the photo-Fenton process and will therefore not be further commented; interested readers can follow the works cited herein [32,56].

Meanwhile, the photo-Fenton reaction achieves a 6-log bacterial population decrease within 90 min, due to enhancements brought by the hydroxyl radical, superoxide and the replenishment of the iron catalyst. In order to compare the bacterial inactivation under various conditions, the pseudo first-order rate constants (k_{app}^{1st}) of reactions were calculated and reported in Table 3. In the presence of iron, and light, the rate constant values for *E. coli* inactivation was increased from $(1.779 \pm 0.143) \times 10^{-4}$ s^{-1} (dark Fenton reaction) to $(1.100 \pm 0.144) \times 10^{-3}$ (Fenton under light). In fact, this value could indicate the capacity of solar light to react with Fe^{3+} species, and regenerating the Fe^{2+} catalyst (Eq. 22) [57]. This kind of catalytic cycle of Fe^{2+} explains the high synergy, which can improve the *E. coli* inactivation in PF process.

Furthermore, the role of oxygen in the presence of iron was investigated (Fig. 6). By purging N_2 into the system and remove all of dissolved oxygen in the presence of Fe^{2+}, the rate of bacterial inactivation was decreased from $(7.144 \pm 0.937) \times 10^{-4}$ s^{-1} to $(2.572 \pm 0.181) \times 10^{-4}$ s^{-1}. This result indicated the critical role of oxygen in this reaction, to generate active species and participating in the catalytic cycle of Fe^{2+}. Or simply put, in "absence" of oxygen, no ROS are expected.

3.4.2. Assessing the photo-Fenton process and its constituents in presence of SR and NR NOM

In order to evaluate the role of NOM in photo-Fenton processes, firstly the reaction was carried out in the presence of different NOM isolates, in absence of H_2O_2. By addition of NOM in the reactors, the loss of iron decreased due to participation of Fe^{2+} in the photo-catalytic cycle. Due to the hydrolysis of the iron salt ($FeSO_4 \rightarrow Fe^{2+} + SO_4^{2-}$), the positively charged iron ion can be adsorbed to the *E. coli* cell wall, or to NOM in the natural water and wastewater [57], as well as produce various complexes such as Fe-NOM, and Fe-*E. coli*. The Fe-NOM complexes have been proposed to exhibit a ligand-to-meal charge transfer (LMCT) in this reaction as the following reactions indicate (Eqs. (23), and (24), and thus improve the *E. coli* inactivation.

$$Fe^{3+} + NOM \rightarrow Fe^{3+}NOM \quad (23)$$

$$Fe^{3+}NOM \xrightarrow{h\nu} Fe^{2+} + NOM_{ox}^{+} \quad (24)$$

The addition of NOM in presence of Fe has increased the bacterial inactivation (Fig. 7) for any of the two isolates (SR, and NR NOM). More specifically, a 30-min reduction has been attained to reduce the bacterial load. The ferrous ions can enter the cell and fuel an intracellular photo-Fenton process [6]. After their oxidation in the bulk, NOM

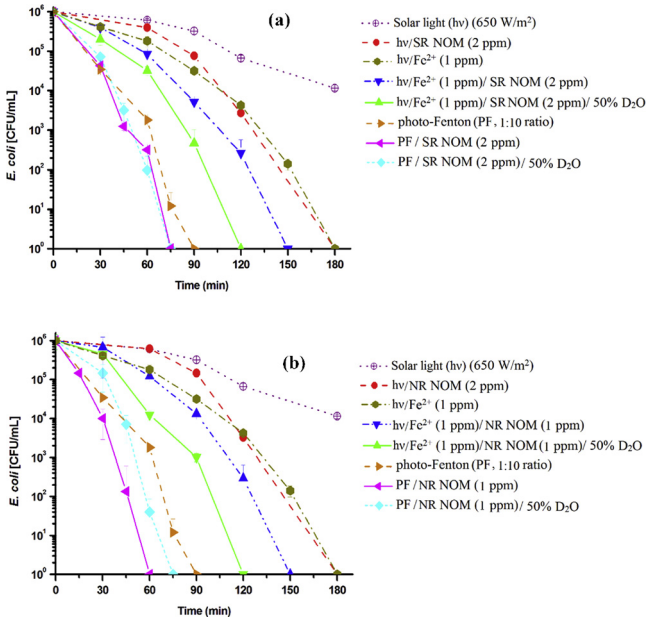

Fig. 7. *E. coli* inactivation in the presence of SR [2 mg/L] (a), and NR [1 mg/L] NOM (b) under combined processes (light Intensity: 650 W/m^2, Fe^{2+} [1 mg/L], H_2O_2 [10 mg/L], and 50% v/v of D_2O).

Table 3
Pseudo-first order rate constant (k_{app}^{1st}) for *E. coli* inactivation under different reaction conditions, and the correlation coefficient of the plots. Reaction condition: Fe^{2+} [1 mg/L], H_2O_2 [10 mg/L], NR NOM [1 mg/L], SR NOM [2 mg/L], D_2O 50% v/v, light intensity: 650 W/m^2.

k_{app}^{1st} (s^{-1})	Standard	Addition of SR NOM	Addition of NR NOM
SODIS (hν)	$(2.101 \pm 0.226) \times 10^{-4}$	$(7.993 \pm 0.861) \times 10^{-4}$	$(8.336 \pm 0.951) \times 10^{-4}$
R^2	0.97759	0.98858	0.98722
Fenton	$(1.779 \pm 0.143) \times 10^{-4}$	–	–
R^2	0.98421		
hν/Fe^{2+}	$(7.144 \pm 0.937) \times 10^{-4}$	$(8.925 \pm 1.139) \times 10^{-4}$	$(9.391 \pm 1.323) \times 10^{-4}$
R^2	0.97514	0.98409	0.9807
hν/Fe^{2+}/D_2O	–	$(9.843 \pm 1.650) \times 10^{-4}$	$(1.000 \pm 0.157) \times 10^{-3}$
R^2		0.972	0.97614
hν/Fe^{2+}/N_2	$(2.572 \pm 0.181) \times 10^{-4}$	–	–
R^2	0.98546		
hν/H_2O_2	$(9.411 \pm 1.895) \times 10^{-4}$	–	–
R^2	0.96176		
PF	$(1.100 \pm 0.144) \times 10^{-3}$	$(1.270 \pm 0.194) \times 10^{-3}$	$(1.970 \pm 0.133) \times 10^{-3}$
R^2	0.97541	0.9664	0.99543
PF/D_2O	–	$(1.670 \pm 0.178) \times 10^{-3}$	$(2.220 \pm 0.081) \times 10^{-3}$
R^2		0.98326	0.99933

carboxylate groups can facilitate the ligands with Fe, to then get Fe^{3+} reduced to Fe^{2+}, due to LMCT and the sacrificial role of NOM. The "in-situ" prepared complex can participate again in the reaction and produce the ferric ion by self-catalytic process [4]. The ferric ion can also pass into the cell and improve the inactivation of bacteria by light, albeit *via* a siderophoric protein action. Due to the oxidation of iron inside the cell and the subsequent interaction with DNA, the rate of inactivation can be increased and LMCT with DNA may happen [6]. In this step, the Fe^{3+} can be converted to Fe^{2+} and use in another cycle. As far as the extracellular Fe^{3+} is concerned, it can bind to the surface of *E. coli* in the bulk, and participate in an LMCT with the bacterial membrane.

Also, by addition of NOM in the presence of iron and H_2O_2 more ROS including $^1O_2$, superoxide and principally, *HO*● can be produced and enhance the rate of *E. coli* inactivation. Fig. 7 (a, and b) illustrates the role of different conditions in bacterial inactivation for SR and NR NOM, respectively. As can be seen, by plain addition of Fe^{2+} into the reaction, the rate constant was increased in the presence of both SR and NR NOM. Table 3 summarizes the apparent first order rate constant values of bacterial inactivation under the various conditions. These results confirm that either NOM or Fe and the subsequent NOM-Fe complexes have an enhancing activity on the kinetics and add further pathways in the mechanism of bacterial inactivation.

According to the obtained values, in the experiments in presence of D_2O (50%) during the photo-Fenton reaction, the rate constant values increased compared with the photo-Fenton process in H_2O. More specifically, the respective value for NR NOM (2.22×10^{-3} s^{-1}) was higher than SR NOM (1.67×10^{-3} s^{-1}), which indicated i) the additional role of singlet oxygen and, ii) the iron complexes action. The obtained results confirmed that the chemical properties of NOM have a critical role in ROS dynamics. These traits are influenced by climate and environment including vegetation, domestic wastewaters and soil [58]. The obtained results indicated that SR NOM is more active in the generation of $^3NOM^*$. By addition of D_2O, the 1st order rate constant of bacterial inactivation in the presence of SR NOM slightly increased; and a 6-log bacterial population decrease was reached at 75 min. This behavior confirmed that the triplet state of NOM ($^3NOM^*$) has an important role in this reaction compared with singlet oxygen ($^1O_2$). On the other hand, the reaction with NR NOM, and D_2O (50%) achieves faster *E. coli* inactivation, within 60 min. This behavior can be related to best performance of NR NOM in the generation of active species, and form iron complexes. By irradiation of solar light not only $^3NOM^*$ and $O1_2$ were obtained but also interaction between NOM and Fe (NR-Fe) can enhance the bacterial inactivation rate. Hence, a question arises in the difference of the NOM origin, and distribution of HA and FA within it.

This point, which warrants further discussion, can be located in the level of modifications NOM can play in solar disinfection, when compared to PF. More specifically, the improvement in kinetics from plain solar irradiation to the enhanced process in presence of (any) NOM isolate is almost 4 times higher. On the contrary, the improvement of PF in presence of NR NOM is only 1.8 times, and can get as low as 1.2 with SR NOM. Similar values are noted for the hv/Fe. As such, it is important to note the interdependence of the success of disinfection in the composition of the NOM present in water, or put differently, the low influence (but beneficial) that has on photo-Fenton. This effect also makes the photo-Fenton a more robust process, when it comes to bacterial inactivation, which is less affected by environmental factors as NOM composition, or else, a less dependent process concerning its effects.

In order to compare more easily the results of the bacterial inactivation observed in the NOM isolates so far, the apparent first order reaction rate constant for experiments containing SRHA and SRFA instead of NOM were calculated and summarized in Fig. 8. According to the obtained results, in fact, both acids enhance the solar inactivation and HA, and FA present almost similar inactivation rates respectively. By addition of HA and FA in the presence of Fe and H_2O_2, due to the higher production of more active species, the efficiency of solar

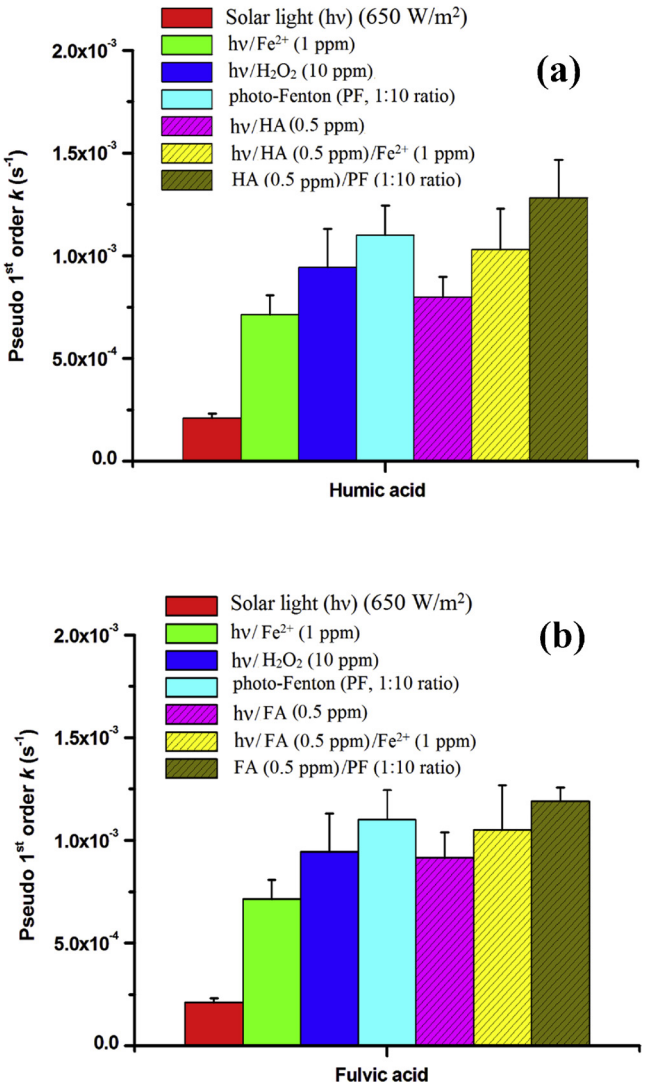

Fig. 8. Kinetic evaluation of *E. coli* inactivation for (a) SR Humic acid (HA), and (b) SR Fulvic acid (FA).

disinfection increased. As also shown, adding HA and FA to the photo-Fenton process decreases the time required to reach a 6-log decrease in bacterial population down to 75, and 90 min, respectively (Figure S9).

Hence, a slightly modified behavior compared to plain solar exposure has been encountered; HA contribute further to the photochemical cycle with the interactions with Fe, and enhance the photo-Fenton process in presence of HA, making it more efficient than the FA-supported. This effect could be an indication of higher amount of carboxylate groups in HA. Nevertheless, similarly to the NOM experiments, the effect of NOM presence in light was significantly higher than photo-Fenton. Hence, the enhancement by NOM is optative, if one would be to rely on PF for water disinfection.

In order to further elucidate the events taking place during solar and photo-Fenton disinfection, the concentration of iron, H_2O_2 and the pH of the solution were monitored and the results for water, water with SRNOM, and with SRHA are presented in Fig. 9. Here it can be readily seen why the presence of NOM enhances inactivation. In principle Fe-NOM complexes are generated, which prevent its precipitation and facilitate its participation in the photo-chemical cycle, as seen by the higher concentrations in presence of organic matter, for a similar H_2O_2 consumption that corresponds to HO● production. Also, SRNOM performed better than SRHA, implying that even if the most photo-active part is HA, the rest of the components play an important part in the

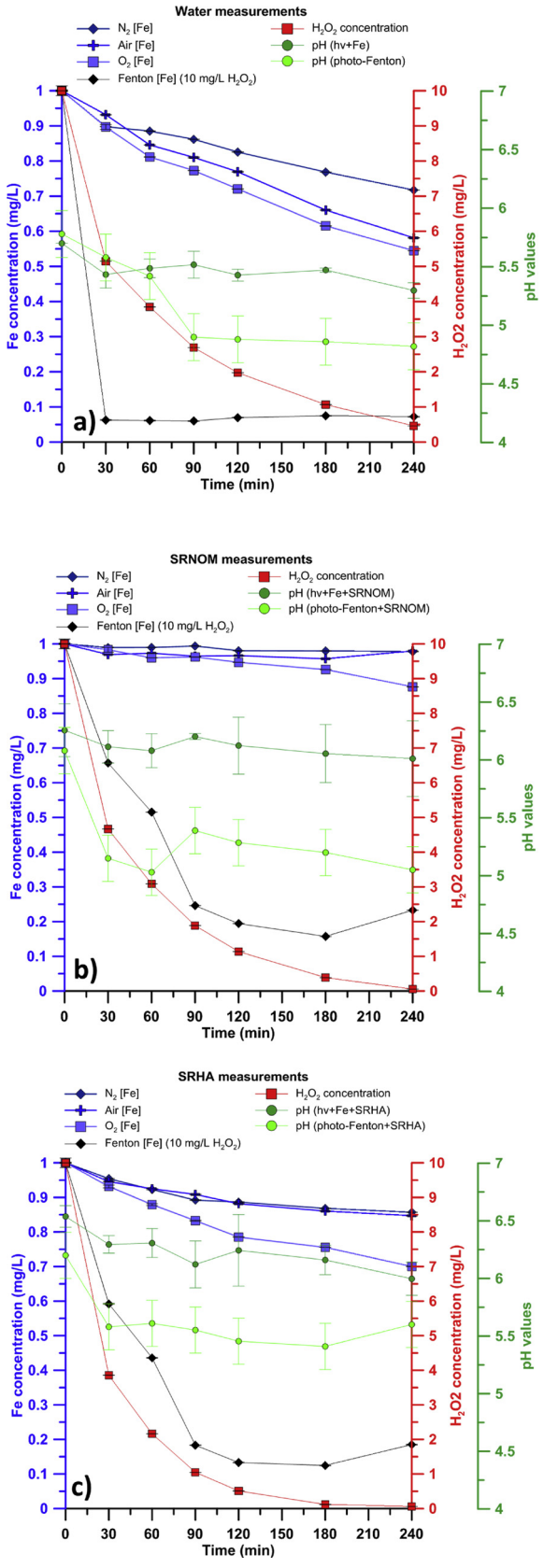

Fig. 9. Fe and H_2O_2 concentration, and pH of the solution in solar-assisted experiments (hv + Fe or photo-Fenton). a) Experiments in MQ water. b) Experiments in presence of 2 mg/L DOC of SRNOM. c) Experiments in presence of 2 mg/L DOC of SRHA. The iron concentrations in the three atmospheres are tested (N_2, normal O_2, saturated O_2) as well as during photo-Fenton (normal O_2). The H_2O_2 concentration corresponds to the photo-Fenton experiment and the average pH values are given grouped for the three atmosphere conditions; the vertical bars here represent the highest/lowest values encountered. The colors of the traces correspond to the colors of the axes.

process. This higher efficiency has been previously encountered in wastewater [51,59], while this higher availability of iron leads to an enhanced photo-Fenton process compared to water, and a slightly lower pH value than SRHA, but remains near-neutral. Finally, in order to summarize all the effects presented, an overall inactivation scheme is hereby presented (Fig. 10), where the prevalent and secondary pathways are summarized.

4. Conclusions

Organic matter in its particulate and dissolved form (NOM) is always present in natural waters. In this work, the interdependence of oxygen, NOM and bacterial inactivation efficiency during solar exposure and the photo-Fenton process was systematically assessed. An effort to dissociate the constituents of the latter, which lead to bacterial inactivation was performed.

Firstly, the concentration of NOM and its effect were assessed. Natural waters present a range of concentrations and the present investigation revealed that up to 5–7 mg/L all solar processes were enhanced, regardless of the NOM origin (autochthonous, SR or allochthonous, NR). As such, what is perceived during solar disinfection assessment, is already the combined effect of the actions. However, the use of humic or fulvic acid (HA/FA) isolates revealed that the photochemical events are more obvious in HA.

When it comes to the photo-chemical production of transient species, our study focused mostly in $^3NOM^*$ and $^1O_2$, as the most prevalent inactivation factors due to NOM. The $^1O_2$ pathway was further assessed in water-free environments (D_2O) or O_2-saturated ones, further enhancing inactivation, and its contribution was quantified with relevance to $^3NOM^*$. Also, the origin of NOM, did demonstrate preferential pathways, namely $^3NOM^*$ for SR and $^1O_2$ for NR organic matter isolates.

In the presence of iron, NOM acquires new pathways and inactivating transients, but the photo-Fenton process assayed only gets enhanced by the NOM-Fe complexes, which allow the process to be carried out more effectively at near-neutral pH, because $HO^{\bullet}$ is the main oxidizing species, which need Fe for its generation. Finally, in these cycles, the difference among HA and FA is not found in the enhancement of the solar disinfection baseline, but in the higher involvement of HA in Fe complexation.

In conclusion, apart from the partial elucidation of the photo-chemical cycle due to the presence of NOM, the environmental significance of this study lies in the view of the solar disinfection process. Its germicidal effect is an outcome of different synergic and antagonistic processes and the efficacy prediction can be performed as a function of the photo-generated transient species according to the type of NOM in water. Photo-Fenton is an exception that doesn't get easily affected; its robustness shows opportunities for application as an enhanced solar disinfection version.

Acknowledgements

The authors would like to thank the Sharif University of Technology, and the Ministry of Science, Research and Technology of the Islamic Republic of Iran for the financial support of Mona Kohantorabi during her research stay in École Polytechnique Fédérale de Lausanne (EPFL), Switzerland. Also, the financial support from China Scholarship Council for Ling Feng during her research stay in École Polytechnique Fédérale de Lausanne (EPFL), Switzerland must be

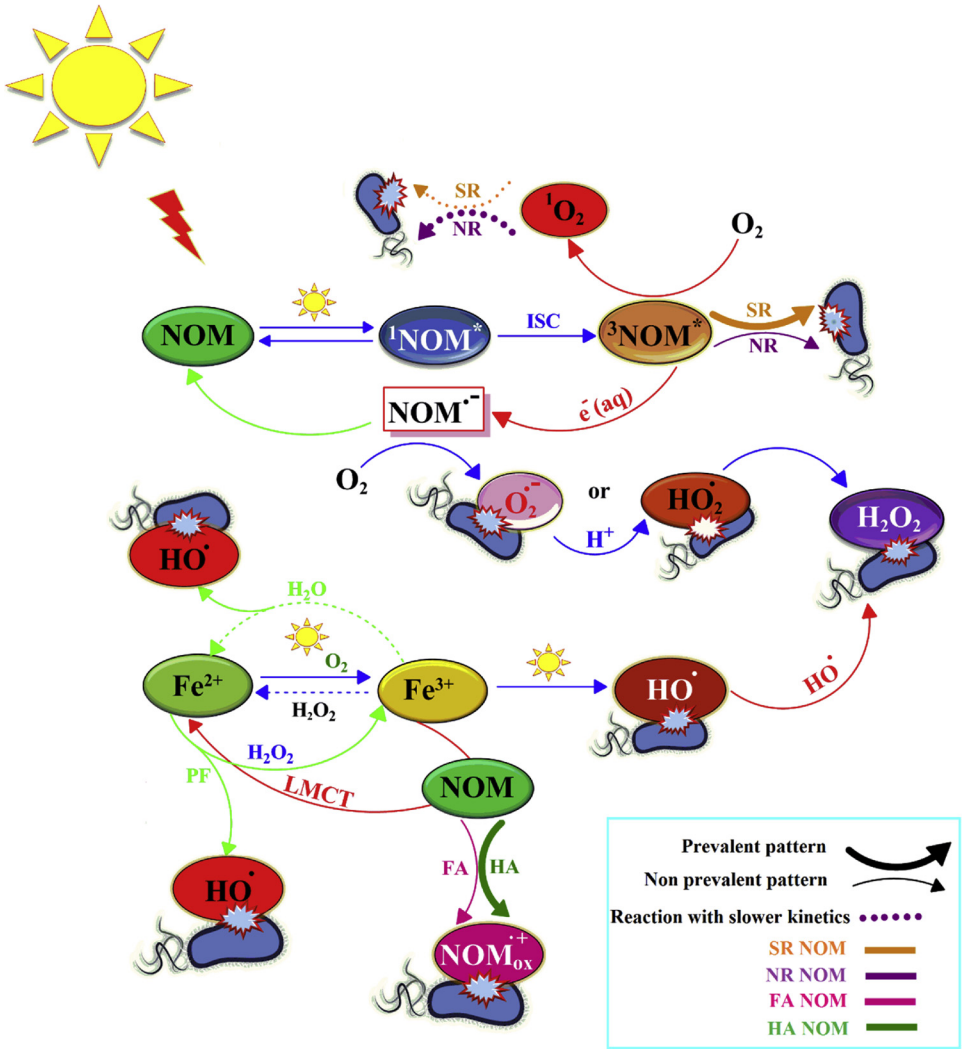

Fig. 10. The proposed integrated mechanism of bacterial inactivation pathways.

acknowledged. Finally, Stefanos Giannakis and Cesar Pulgarin would like to acknowledge the financial support through the European project WATERSPOUTT H2020-Water-5c-2015 (GA 688928) and the Swiss State Secretariat for Education, Research and Innovation (SEFRI-WATERSPOUTT, No.: 588141).

Appendix A. Supplementary data

Supplementary material related to this article can be found, in the online version, at doi:https://doi.org/10.1016/j.apcatb.2018.12.012.

References

[1] K.G. McGuigan, R.M. Conroy, H.J. Mosler, M. du Preez, E. Ubomba-Jaswa, P. Fernandez-Ibanez, Solar water disinfection (SODIS): a review from bench-top to roof-top, J. Hazard. Mater. 235 (236) (2012) 29–46, https://doi.org/10.1016/j.jhazmat.2012.07.053.

[2] T. Clasen, W.-P. Schmidt, T. Rabie, I. Roberts, S. Cairncross, Interventions to improve water quality for preventing diarrhoea: systematic review and meta-analysis, Bmj 334 (2007) 782.

[3] G. Hutton, L. Haller, J. Bartram, Global cost-benefit analysis of water supply and sanitation interventions, J. Water Health 5 (2007) 481–502.

[4] S. Giannakis, Analogies and differences among bacterial and viral disinfection by the photo-Fenton process at neutral pH: a mini review, Environ. Sci. Pollut. Res. (2018), https://doi.org/10.1007/s11356-017-0926-x.

[5] M. Figueredo-Fernández, S. Gutierrez-Alfaro, A. Acevedo-Merino, M.A. Manzano, Estimating lethal dose of solar radiation for enterococcus inactivation through radiation reaching the water layer. Application to Solar Water Disinfection (SODIS), Sol. Energy 158 (2017) 303–310.

[6] S. Giannakis, M.I. Polo López, D. Spuhler, J.A. Sánchez Pérez, P. Fernández Ibáñez, C. Pulgarin, Solar disinfection is an augmentable, in situ-generated photo-Fenton reaction—part 1: a review of the mechanisms and the fundamental aspects of the process, Appl. Catal. B Environ. 199 (2016), https://doi.org/10.1016/j.apcatb.2016.06.009.

[7] M. Berney, H.U. Weilenmann, A. Simonetti, T. Egli, Efficacy of solar disinfection of Escherichia coli, Shigella flexneri, Salmonella typhimurium and Vibrio cholerae, J. Appl. Microbiol. 101 (2006) 828–836, https://doi.org/10.1111/j.1365-2672.2006.02983.x.

[8] S. Giannakis, E. Darakas, A. Escalas-Cañellas, C. Pulgarin, Temperature-dependent change of light dose effects on E. Coli inactivation during simulated solar treatment of secondary effluent, Chem. Eng. Sci. 126 (2015), https://doi.org/10.1016/j.ces.2014.12.045.

[9] M. Castro-Alférez, M.I. Polo-López, J. Marugán, P. Fernández-Ibáñez, Mechanistic modeling of UV and mild-heat synergistic effect on solar water disinfection, Chem. Eng. J. 316 (2017) 111–120.

[10] B.M. Voelker, F.M.M. Morel, B. Sulzberger, Iron redox cycling in surface waters: effects of humic substances and light, Environ. Sci. Technol. 31 (1997) 1004–1011, https://doi.org/10.1021/es9604018.

[11] W. Wang, O.C. Zafiriou, I.Y. Chan, R.G. Zepp, N.V. Blough, Production of hydrated electrons from photoionization of dissolved organic matter in natural waters, Environ. Sci. Technol. 41 (2007) 1601.

[12] E.M. Thurman, R.L. Malcolm, Preparative isolation of aquatic humic substances, Environ. Sci. Technol. 15 (1981) 463–466.

[13] G. McKay, K.D. Couch, S.P. Mezyk, F.L. Rosario-Ortiz, Investigation of the coupled effects of molecular weight and charge-transfer interactions on the optical and photochemical properties of dissolved organic matter, Environ. Sci. Technol. 50 (2016) 8093–8102.

[14] G.R. Aiken, H. Hsu-Kim, J.N. Ryan, Influence of Dissolved Organic Matter on the Environmental Fate of Metals, Nanoparticles, and Colloids, (2011).

[15] Y. Chen, C. Hu, X. Hu, J. Qu, Indirect photodegradation of amine drugs in aqueous solution under simulated sunlight, Environ. Sci. Technol. 43 (2009) 2760–2765, https://doi.org/10.1021/es803325j.

[16] K. Kadir, K.L. Nelson, Sunlight mediated inactivation mechanisms of Enterococcus faecalis and Escherichia coli in clear water versus waste stabilization pond water, Water Res. 50 (2014) 307.
[17] J.T. Jasper, M.T. Nguyen, Z.L. Jones, N.S. Ismail, D.L. Sedlak, J.O. Sharp, R.G. Luthy, A.J. Horne, K.L. Nelson, Unit process wetlands for removal of trace organic contaminants and pathogens from municipal wastewater effluents, Environ. Eng. Sci. 30 (2013) 421–436.
[18] E.A. Serna-Galvis, J.A. Troyon, S. Giannakis, R.A. Torres-Palma, C. Minero, D. Vione, C. Pulgarin, Photoinduced disinfection in sunlit natural waters: measurement of the second order inactivation rate constants between E. Coli and photogenerated transient species, Water Res. 147 (2018) 242–253, https://doi.org/10.1016/j.watres.2018.10.011.
[19] C.S. Foote, Definition of type I and type II photosensitized oxidation, Photochem. Photobiol. 54 (1991) 659.
[20] C.A. Murray, S.A. Parsons, Removal of NOM from drinking water: fenton's and photo-Fenton's processes, Chemosphere. 54 (2004) 1017–1023, https://doi.org/10.1016/j.chemosphere.2003.08.040.
[21] D.C. Waggoner, A.S. Wozniak, R.M. Cory, P.G. Hatcher, The role of reactive oxygen species in the degradation of lignin derived dissolved organic matter, Geochim. Cosmochim. Acta 208 (2017) 171–184.
[22] M. Marjanovic, S. Giannakis, D. Grandjean, L.F. de Alencastro, C. Pulgarin, Effect of MM Fe addition, mild heat and solar UV on sulfate radical-mediated inactivation of bacteria, viruses, and micropollutant degradation in water, Water Res. 140 (2018), https://doi.org/10.1016/j.watres.2018.04.054.
[23] S. Giannakis, S. Rtimi, C. Pulgarin, Light-assisted advanced oxidation processes for the elimination of chemical and microbiological pollution of wastewaters in developed and developing countries, Molecules 22 (2017), https://doi.org/10.3390/molecules22071070.
[24] S. Arzate, J.L.G. Sánchez, P. Soriano-Molina, J.L.C. López, M.C. Campos-Mañas, A. Agüera, J.A.S. Pérez, Effect of residence time on micropollutant removal in WWTP secondary effluents by continuous solar photo-Fenton process in raceway pond reactors, Chem. Eng. J. 316 (2017) 1114–1121.
[25] S. Giannakis, M.I.P. López, D. Spuhler, J.A.S. Pérez, P.F. Ibáñez, C. Pulgarin, Solar disinfection is an augmentable, in situ-generated photo-Fenton reaction-Part 2: a review of the applications for drinking water and wastewater disinfection, Appl. Catal. B Environ. 198 (2016), https://doi.org/10.1016/j.apcatb.2016.06.007.
[26] S. Giannakis, C. Ruales-Lonfat, S. Rtimi, S. Thabet, P. Cotton, C. Pulgarin, Castles fall from inside: evidence for dominant internal photo-catalytic mechanisms during treatment of Saccharomyces cerevisiae by photo-Fenton at near-neutral pH, Appl. Catal. B Environ. 185 (2016), https://doi.org/10.1016/j.apcatb.2015.12.016.
[27] K.L. Nelson, A.B. Boehm, R.J. Davies-Colley, M.C. Dodd, T. Kohn, K.G. Linden, Y. Liu, P.A. Maraccini, K. McNeill, W.A. Mitch, Sunlight-mediated inactivation of health-relevant microorganisms in water: a review of mechanisms and modeling approaches, Environ. Sci. Process. Impacts 20 (2018) 1089–1122.
[28] S. Halladja, A. ter Halle, J.-P.P. Aguer, A. Boulkamh, C. Richard, Inhihition of humic substances mediated photooxygenation of furfuryl alcohol by 2,4,6-trimethylphenol. Evidence for reactivity of the phenol with humic triplet excited states, Environ. Sci. Technol. 41 (2007) 6066–6073.
[29] V. Romero, S. Acevedo, P. Marco, J. Giménez, S. Esplugas, Enhancement of Fenton and photo-Fenton processes at initial circumneutral pH for the degradation of the β-blocker metoprolol, Water Res. 88 (2016) 449–457.
[30] A.-G. Rincón, C. Pulgarin, Comparative evaluation of Fe3+ and TiO2 photoassisted processes in solar photocatalytic disinfection of water, Appl. Catal. B Environ. 63 (2006) 222–231, https://doi.org/10.1016/j.apcatb.2005.10.009.
[31] J.J. Pignatello, E. Oliveros, A. MacKay, Advanced oxidation processes for organic contaminant destruction based on the fenton reaction and related chemistry, Crit. Rev. Environ. Sci. Technol. 36 (2006) 1–84, https://doi.org/10.1080/10643380500326564.
[32] D. Spuhler, J.A. Rengifo-Herrera, C.C. Pulgarin, J. Andrés Rengifo-Herrera, C.C. Pulgarin, The effect of Fe2+, Fe3+, H202 and the photo-Fenton reagent at near neutral pH on the solar disinfection (SODIS) at low temperatures of water containing Escherichia coli K12, Appl. Catal. B 96 (2010) 126–141, https://doi.org/10.1016/j.apcatb.2010.02.010.
[33] P. Villegas- Guzman, S. Giannakis, S. Rtimi, D. Grandjean, M. Bensimon, L.F.L.F. De Alencastro, R. Torres-Palma, C. Pulgarin, A green solar photo-Fenton process for the elimination of bacteria and micropollutants in municipal wastewater treatment using mineral iron and natural organic acids, Appl. Catal. B Environ. 219 (2017) 538–549, https://doi.org/10.1016/j.apcatb.2017.07.066.
[34] R. Khaengraeng, R.H. Reed, Oxygen and photoinactivation of Escherichia coli in UVA and sunlight, J. Appl. Microbiol. 99 (2005) 39–50.
[35] R.H. Reed, The inactivation of microbes by sunlight: solar disinfection as a water treatment process, Adv. Appl. Microbiol. 54 (2004) 333–365.
[36] T. Kohn, K.L. Nelson, Sunlight-mediated inactivation of MS2 coliphage via exogenous singlet oxygen produced by sensitizers in natural waters, Environ. Sci. Technol. 41 (2007) 192–197.
[37] J. Ndounla, S. Kenfack, J. Wéthé, C. Pulgarin, Relevant impact of irradiance (vs. dose) and evolution of pH and mineral nitrogen compounds during natural water disinfection by photo-Fenton in a solar CPC reactor, Appl. Catal. B Environ. 148 (149) (2014) 144–153, https://doi.org/10.1016/j.apcatb.2013.10.048.
[38] C.M. Sharpless, N.V. Blough, The importance of charge-transfer interactions in determining chromophoric dissolved organic matter (CDOM) optical and photochemical properties, Environ. Sci. Process. Impacts 16 (2014) 654.
[39] N. Walpen, M.H. Schroth, M. Sander, Quantification of phenolic antioxidant moieties in dissolved organic matter by flow-injection analysis with electrochemical detection, Environ. Sci. Technol. 50 (2016) 6423–6432.
[40] R.M. Dalrymple, A.K. Carfagno, C.M. Sharpless, Correlations between dissolved organic matter optical properties and quantum yields of singlet oxygen and hydrogen peroxide, Environ. Sci. Technol. 44 (2010) 5824–5829.
[41] A.C. Gerecke, S. Canonica, S.R. Müller, M. Schärer, R.P. Schwarzenbach, Quantification of dissolved natural organic matter (DOM) mediated phototransformation of phenylurea herbicides in lakes, Environ. Sci. Technol. 35 (2001) 3915.
[42] A.L. Boreen, B.L. Edhlund, J.B. Cotner, K. McNeill, Indirect photodegradation of dissolved free amino acids: the contribution of singlet oxygen and the differential reactivity of DOM from various sources, Environ. Sci. Technol. 42 (2008) 5492–5498.
[43] T. Maisch, J. Baier, B. Franz, M. Maier, M. Landthaler, R.-M. Szeimies, W. Bäumler, The role of singlet oxygen and oxygen concentration in photodynamic inactivation of bacteria, Proc. Natl. Acad. Sci. 104 (2007) 7223–7228.
[44] D.G. Jay, H. Keshishian, Laser inactivation of fasciclin I disrupts axon adhesion of grasshopper pioneer neurons, Nature. 348 (1990) 548.
[45] B.A. Griffin, S.R. Adams, R.Y. Tsien, Specific covalent labeling of recombinant protein molecules inside live cells, Science 80- (281) (1998) 269–272.
[46] F. Wilkinson, W.P. Helman, A.B. Ross, Rate constants for the decay and reactions of the lowest electronically excited singlet state of molecular oxygen in solution - an expanded and revised compilation, J. Phys. Chem. Ref. Data 24 (1995) 663–677.
[47] P.R. Ogilby, Singlet oxygen: there is indeed something new under the sun, Chem. Soc. Rev. 39 (2010) 3181–3209.
[48] W.R. Haag, J. Hoigné, Singlet oxygen in surface waters. 3. Photochemical formation and steady-state concentrations in various types of waters, Environ. Sci. Technol. 20 (1986) 341.
[49] C.M. Sharpless, Lifetimes of triplet dissolved natural organic matter (DOM) and the effect of NaBH4 reduction on singlet oxygen quantum yields: implications for DOM photophysics, Environ. Sci. Technol. 46 (2012) 4466, https://doi.org/10.1021/es300217h.
[50] J. Marugán, R. van Grieken, C. Sordo, C. Cruz, Kinetics of the photocatalytic disinfection of Escherichia coli suspensions, Appl. Catal. B Environ. 82 (2008) 27–36, https://doi.org/10.1016/j.apcatb.2008.01.002.
[51] S. Giannakis, S. Liu, A. Carratalà, S. Rtimi, M. Bensimon, C. Pulgarin, Effect of Fe (II)/Fe(III) species, pH, irradiance and bacterial presence on viral inactivation in wastewater by the photo-Fenton process: kinetic modeling and mechanistic interpretation, Appl. Catal. B Environ. 204 (2017), https://doi.org/10.1016/j.apcatb.2016.11.034.
[52] E. Appiani, R. Ossola, D.E. Latch, P.R. Erickson, K. McNeill, Aqueous singlet oxygen reaction kinetics of furfuryl alcohol: effect of temperature, pH, and salt content, Environ. Sci. Process. Impacts 19 (2017) 507–516.
[53] M. Minella, S. Giannakis, A. Mazzavillani, V. Maurino, C. Minero, D. Vione, Phototransformation of Acesulfame K in surface waters: comparison of two techniques for the measurement of the second-order rate constants of indirect photodegradation, and modelling of photoreaction kinetics, Chemosphere. 186 (2017), https://doi.org/10.1016/j.chemosphere.2017.07.128.
[54] E. Desmond-Le Quéméner, T. Bouchez, A thermodynamic theory of microbial growth, ISME J. 8 (2014) 1747.
[55] S. Giannakis, M. Voumard, S. Rtimi, C. Pulgarin, Bacterial disinfection by the photo-Fenton process: Extracellular oxidation or intracellular photo-catalysis? Appl. Catal. B Environ. 227 (2018), https://doi.org/10.1016/j.apcatb.2018.01.044.
[56] F. Sciacca, J.A. Rengifo-Herrera, J. Wéthé, C. Pulgarin, Dramatic enhancement of solar disinfection (SODIS) of wild Salmonella sp. In PET bottles by H 2 O 2 addition on natural water of Burkina Faso containing dissolved iron, Chemosphere 78 (2010) 1186–1191.
[57] A. Armanious, M. Münch, T. Kohn, M. Sander, Competitive co-adsorption dynamics of viruses and dissolved organic matter to positively charged sorbent surfaces, Environ. Sci. Technol. (2016).
[58] M. Fujii, E. Otani, Photochemical generation and decay kinetics of superoxide and hydrogen peroxide in the presence of standard humic and fulvic acids, Water Res. 123 (2017) 642–654.
[59] S. Giannakis, S. Liu, A. Carratalà, S. Rtimi, M. Talebi Amiri, M. Bensimon, C. Pulgarin, Iron oxide-mediated semiconductor photocatalysis vs. heterogeneous photo-Fenton treatment of viruses in wastewater. Impact of the oxide particle size, J. Hazard. Mater. 339 (2017), https://doi.org/10.1016/j.jhazmat.2017.06.037.